Scholars Journal of Science and Technology
Published By Scholar Indexing Society
E-ISSN: 2955-7844
DOI Url: http://doi.org/10.53075/ljmsirq/56646656
Journal Homepage: https://globalweb1.com/index.php/ojs
Volume 3, Number 4, pp. 796-812

A Hybrid Multi-Class Classification of Alzheimer Disease Based on Operative Deep Learning Techniques: Xception-Fractalnet

Chukwuma Chinaza Adaobi[1], Atianashie Miracle A.[2], Mathias Justice Akanzabwon Asaarik[3], Nyamike A Miezah[4], and James Kwabena Odum[5]

[1,2,3,5] Catholic University of Ghana, Fiapre, P.O. Box 363, Sunyani
[4] Preceptor, Sunyani Municipal Hospital, Sunyani, Bono Region Ghana

Corresponding author: Chukwuma Chinaza Adaobi, email: **chinazaadaobi26@gmail.com**

Date Received: July 27, 2022 **Date Published:** September 21, 2022

Abstract: Alzheimer's disease (AD) is a type of dementia that affects people as they get older and is one of the most frequent memory depletion diseases. Early-stage AD identification is essential for preventing and intervening the disease development. But it is a challenging task due to the complex structure of brain and its functions. Hence, the research on AD has increased recently. Therefore in this paper, an effective hybrid Xception and Fractalnet based deep learning framework is implemented to classify the stages of AD into five classes. To increase the performance of the classifier, an effective pre-processing methods and Unet++ based segmentation technique are applied on Magnetic Resonance Imaging (MRI) images gathered from ADNI dataset. The performance of the proposed approach is analysed based on Recall, precision and accuracy metrics. The investigation results shows that the proposed technique have the capacity to attain 98.30% recall, 99.72% precision, and 99.06% accuracy in multiclass classification. The results indicate that the proposed techniques combined with MRI images can be utilized to categorize forecast neurodegenerative brain illnesses like AD.

Keywords: Deep learning, Fractalnet, Xception, Unet++, Alzheimer's disease, Magnetic Resonance (MRI)

DOI: 10.53075/ljmsirq/56646656

1. Introduction

Alzheimer's disease (AD) is an illness that affects the brain and causes it to deteriorate. This is a neurological state. In this, the cells in the brains are dying, causing in cognitive impairment and memory loss. It is one of the most frequent types of dementia, and it has a significant detrimental influence on social and personal lives of peoples [1-3]. The memory related neurological illness is commonly known as dementia and AD is most frequent kind. As per the 2015 World Alzheimer's information, around 50 million humans are affected by dementia, with AD accounting for 70–80% of occurrences. According to estimates, 131.5 million individuals worldwide would be affected by AD in 2050 [4, 5]. The global prevalence of AD is worrying because every three seconds one person is affected by this disease.

Chemicals, head injuries, genetic and environmental factors are the most important causes of AD. Behaviour and mood instability, communication and recognition problems, learning issues, and memory loss are all common signs of AD [6-8]. It triggers brain cell's death, resulting in thinking, memory, and cognitive impairment. It progresses over time and is labelled as a pre-clinical stage. The rate at which this disease progresses varies from patient to patient, but it has a terrible outcome. It produces a behavioural abnormality that affects the patient's social functionality [9-11]. The normal onset and signs of this illness appear beyond the age of 65, however it can develop earlier in life and the symptoms may not appear until this age.

The hippocampus and cerebral cortex sizes are reduced in AD patient's brain. Even though, the ventricle's size is increased in the brain. If the hippocampus size is reduced, the episodic and spatial memory parts are damaged. It also decreases the connectivity among the body and brain [12-14]. Cell death and damage of

synapses and neuron endings occur as a result of hippocampus shrinkage. Communication problems in short-term memory, judgement and planning have been found as a result of neuronal uncertainty.

AD is a multiclass classification issue, the majority of existing research is focused on binary classification, in which either an individual has AD or does not. This is unimportant in AD diagnosis because the stage of the disease is more crucial [15-17]. Different clinical examinations are required for the diagnosis of AD, resulting in a vast amount of data samples. As a result, manual data analysis for detecting AD stages is not possible. Many Computer-Aided Diagnosis Systems (CADS) have been created by the researchers to accurately detect and classify the retrieved aspects linked to AD. But more time and effort of human experts is required to process the extracted features.

Various studies employed a variety of machine learning algorithms to categorise Alzheimer's disease using neuroimaging data. On the other hand, conventional machine learning algorithms necessitate the human extraction of features prior to categorization. User defined features based approaches have drawbacks. Because it is failure to select the unique features related to the problem [18-20]. For automatic feature extraction and analysis of brain data, deep learning techniques are recently utilized in the area of neuro-imaging with the use of graphical processing units and improved processing power. The deep learning models are attained best results due to its automatic feature extraction ability.

As per the drawback of traditional methods in classification and feature extraction, in this paper, an effective hybrid Xception-Fractalnet based deep learning technique is proposed for Alzheimer disease classification system. It classifies the AD into 5 classes namely Cognitively Normal (CN), Late Mild Cognitive Impairment (LMCI), Early Mild Cognitive Impairment (EMCI), Mild Cognitive Impairment (MCI), and Alzheimer Disease (AD). Moreover, Unet++ based effective segmentation network is applied to improve the classification system's performance and identify AD in the beginning.

The important contributions of this paper are listed in the following three aspects,

- To propose Unet++ based deep learning technique for effective segmentation of MRI brain images.
- To propose a hybrid Xception-Fractalnet based architecture for feature extraction and classification of AD classes.
- Standard approaches are used to conduct a comparative analysis in order to validate the suggested framework. The proposed technique beats earlier methods and delivers superior classification results.

The remaining part of this paper is organized as follows: In Section 2, the related work about AD classification is discussed. In Section 3, the procedure and the key technology of the proposed approach are described. The evaluation metrics and experimental of the approach are shown in Section 4 and conclusion is drawn in the last Section.

2. Literature Review

Buvaneswari and Gayathri [21] performed an AD segmentation and classification process. For this they implemented the skull stripping as the preprocessing operation on dataset. Then segnet based segmentation was conducted to identify the features of the AD patient's brain parts. Afterwards, Resnet-101 based classification network is implemented to perform the classification process. They take cerebrospinal fluid, hippocampus, cortex thickness, gyri and sulci contour, cortex surface, white matter, and grey matter are the seven features which were extracted by the segnet. To analyse the effectiveness of the technique, accuracy, precision, specificity and sensitivity metrics were used.

For AD classification, AbdulAzeem et al. [22] presented a CNN based end to end framework. They classified both binary and multiclass classification. Five layers were included in this framework. The data acquisition was performed by the initial layer and the data augmentation and thresholding were performed in the second layer to improve the performance of training datasets. The cross validation technique was implemented to train the CNN network in the third layer. And finally, the CNN was implemented in fourth a\layer and the result was obtained in the final layer. For optimization process, Adam optimizer was implemented and the network weights were assigned by the Glorot Uniform weight initializer. For performance assessment, accuracy, precision and recall metrics were used on ADNI dataset and compared with existing state of art techniques.

Turkson et al. [23] proposed spiking deep CNN architecture for three binary classification of AD such as NC vs. MCI, AD vs. MCI and AD vs. NC. Initially, the MRI images were pre-trained by the unsupervised convolutional Spiking Neural Networks. Then the output of this network was processed by the supervised deep CNN for classification process. The authors evaluate their techniques based on the standard performance metrics and compared the result with existing techniques such as Naïve Bayes, K-nearest neighbour (KNN), Support Vector Machine (SVM), Random Forest (RF), 3D CNN and sparse auto encoders.

Amini et al. [24] conducted the experiment with various machine learning techniques like RF, linear discrimination analysis (LDA), SVM, decision tree (DT), KNN. To identify the severity of the AD was analysed by the CNN framework. They utilized ADNI dataset for this research. For feature extraction, multitask techniques were implemented. Moreover, the Mini-Mental State Examination score was used to calculate the severity of the disease. This score includes sever, moderate, mild and low categories.

To recognize and classify the stages of AD, Al-Adhaileh [25] implemented Restnet50 and AlexNet 19 based deep neural network methods. The author collected the MRI images from the kaggle website for experimental evaluation. In this study, both binary (MCI-CN, AD-CN and AD-MCI) and multi class classification (AD-MCI and CN) were conducted. For performance assessment, Accuracy, Sensitivity, specificity and AUC metrics were used and compared with existing techniques.

Xu et al. [26] developed modified Tresnet based deep learning technique to recognize three stages like NC, MCI and AD. Initially, in the pre-processing stage, skull removing process was performed by the FMRIB Software Library (FSL) software with batch processing. Then the MRI images were segmented into white matter, grey matter and Cerebro Spinal Fluid with the use of the he SPM + cat12 tool kits in MATLAB. Finally, the segmented grey matter was taken by the modified Tresnet to classify the stages of AD.

Basheera and Ram [27] modified the CNN architecture with the inception blocks to perform the classification task. These inception blocks were used to extract the deep features from the segmented grey matter slices. For grey matter segmentation, they implemented the enhanced independent component analysis technique. For classification process, they choose particular informative slices from the whole volume MRI images with the use of the entropy. Then the pre-processing was conducted before the segmentation process. In this process, the unwanted tissues from the slices were removed using the skull stripping technique. Finally, the results were analysed using the standard performance metrics and it is compared with existing state of art techniques.

3. Material and Methods

The working procedure of the proposed approach is detailed in this section. The algorithm of the proposed framework is based on five basic steps. The first stage is data pre-processing and augmentation, the second stage is input image segmentation, and the third and fourth stages are feature extraction and dementia classification. Initially, the input data are acquired from the ADNI dataset. Then the pre-processing methods are implemented to eliminate noise and artefacts from data. Pre-processed image is then given into Unet++ based architecture for the segmentation of white matter, grey matter, hippocampus and cerebrospinal fluid. Afterwards, feature extraction and classification of AD is performed by Xception and fractal net based deep learning technique. This technique classifies the AD into 5 classes. They are Cognitively Normal (CN), Late Mild Cognitive Impairment (LMCI), Early Mild Cognitive Impairment (EMCI), Mild Cognitive Impairment (MCI), and Alzheimer Disease (AD). The system architecture of this proposed work is shown in figure 1.

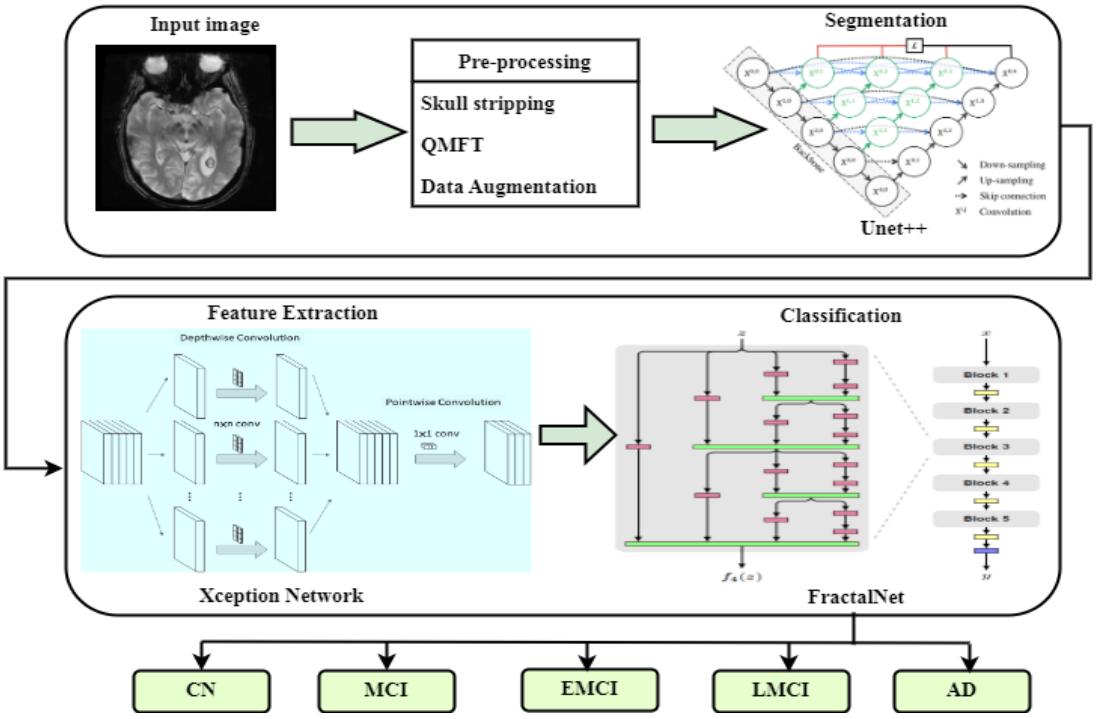

Figure 1: System architecture of proposed system

3.1 Pre-processing

In image processing, pre-processing is the significant phase for smoothing, noise removal and enhancement of images. In this paper, skull stripping technique is implemented in the pre-processing stage to remove the skull in the brain. Because it is not part of the region of interest. Hence skull stripping will help to obtain the better results. Afterwards, the quantum matched-filter technique (QMFT) is applied to remove the low level noise from the image. In this procedure, the essential and specific image features are separated by the active contour. Due to this the unwanted information like noise are removed. Local thresholds can simultaneously identify extensive details by combining small and extensive features and reading all columns and rows diagonally and linearly. Quantum reaches QMFT, which allows for the reduction of noise in MRI images. In addition, various data augmentations like shearing, flipping, rotation (45°) and brightness improvement are performed. Due to this, the amount of database images has increased.

3.2 Segmentation:

For AD classification, the segmentation of cerebrospinal fluid, hippocampus, white matter, and grey matter regions of the brain are most significant part. For this purpose, Unet++ network is adapted and trained to segregate the above mentioned brain regions from pre-processed images. To improve the process of segmentation, the dense block and convoltional layers are provided among the decoder and encoder. Compared to the Unet model, the unet++ architecture has some additions like deep supervision, dense skip connections and redesigned skip pathways. This architecture contains convolution units, skip connections among convolution units, up-sampling and down sampling modules. Each node in this network receives the skip connections at the same level from all convolution units.

Initially, the pre-processed image is given as the input to the Unet++. The input image is then convolved by a convolution layer in the encoder path to obtain the feature map. This feature map passes through the skip routes and is sent to the decoder path's corresponding convolution. Three convolution layers into a dense convolution block are appeared in the skip pathway among the corresponding encoder and decoder nodes. Here, a concatenation layer is preceded into the each convolution layer which combines the output from the up-sampled result of the lower dense block with the corresponding dense block's previous convolution layer. The loss of semantic information among the two pathways is minimised with this structure. Down-sampling is done in the encoder path using a maximum pooling operation with a 2 kernel size and 1 stride. The feature map is half the size with this window and stride arrangement. The features are effectively extracted from the image using down-

sampling operation in encoder path and the up-sampling is employed in the decoder pipeline to double the size of the feature map. Lastly, the segmentation mask is generated based on the final feature maps.

Let us assume that the output of node $y^{i,j}$ is denoted by $y^{i,j}$, where i and j denotes the down sampling and convolution layers respectively. The down sampling layers are appeared in the encoder path and the convolution layers are appeared in the skip pathway. The generation of feature maps by $y^{i,j}$ is described as

$$x^{i,j} = \begin{cases} A(y^{i-1,j}), & j = 0 \\ A[[y^{(i,k)}]_{k=0}^{j-1}, u(y^{i+1,j-1})]), & j > 0 \end{cases} \quad (1)$$

Here, the activation function associated with the 1-D convolution operation is represented by A(.), the up-sampling layer is denoted by u(·) and [·] represents the operation of concatenation. Nodes with level j = 0 received only one input from the encoder's preceding layer, whereas nodes with level j > 0 received j + 1 inputs from both the up-sampling layer and skip connections. It's important to note that the activation function is scaled exponential linear units (SeLUs) rather than ReLU, which allows for stronger regularisation approaches and more robust learning.

$$f(y) = \lambda \begin{cases} y, & y > 0 \\ \alpha(\exp(y) - 1), & y \le 0 \end{cases} \quad (2)$$

In this model, the deep supervision method is used to force the decoder blocks' outputs to produce a valid segmentation map. Furthermore, the Unet++ training process's loss function is based on the loss of categorical cross-entropy:

$$loss = -\sum_{i=1}^{k} z_i \log(z_i) \quad (3)$$

Here, z_i is the proportion of classes belonging to class i and k is the number of classes.

3.3 Feature Extraction:

The segmented image is given as an input to the xception framework for feature extraction. The Xception architecture is a modified version of the Inception architecture that uses Depth-wise separable convolutional modules instead of Inception modules. The feature extraction is formed by 36 convolutional layers which are separated into 14 modules in the Xception architecture. Each of the modules is surrounded by linear residual connections (excluding the last and first modules).

To extract features, the segmented pictures are first fed into the convolutional kernels of (3, 3, 64) and (3, 3, 128). The convolution layers' calculations are as follows:

$$x_j^l = f(u_j^l) \quad (4)$$

$$u_j^l = \sum_{i \in M_j} x_i^{l-1} * k_{i,j}^l + b_j^l \quad (5)$$

Here, b^l denotes the offset parameter, the output of l^{th} convolutional channel of the j^{th} convolutional layer is denoted by x_j^l and the net activation of this channel is denoted by u_j^l, which is convolved and offset by the preceding x_i^{l-1} owned.

Second, the depthwise separable convolution is used to extract more features from the feature maps. To decrease the calculation complexity and the amount of parameters, depthwise separable convolution is utilised. The connection layer then receives the produced two-dimensional feature map as input.

$$x^l = f(u^l) \quad (6)$$

$$u^l = w^l x^{l-1} + b^l \tag{7}$$

Here, the threshold offset term denoted by b^l and the fully connected l^{th} layer's weight coefficient is denoted by w^l. The gradient descent approach is then used to change the training error reduction's direction.

$$\delta^l = \frac{\partial E}{\partial u^l} \tag{8}$$

Here, the variations among actual output and desired output's square are represented by E and the squared function error with a change in u^l is denoted by δ^l. Finally, the feature map of the connected layer yields a 2048-dimensional feature vector. For classification, the feature vector will be fed into Fractalnet.

3.4 Classification:

In this work, the classification of AD is conducted based on Fractalnet architecture. The feature vector obtained from the xception network is given as the input to the fractalnet for classification. In this network, five fractal blocks and pooling layer are consequently arranged. $Fb_C(N)$ represents the fractal block where C represents the number of column in the block. In this work, FractalNet with two columns are used. Therefore, in each fractal block, the number of convolution layer is $2^C - 1 = 2^2 - 1 = 3$. $B*2^C - 1$ is the overall depth of the convolution layer, here number of fractal blocks are denoted by B. Because fractal architecture uses 5 fractal blocks, the entire amount of convolution layers in the framework is 3*no of fractal blocks = 3 * 5 = 15. In addition, the results from this shallow network are substantially faster.

The base function of this architecture contains convolution layer, batch normalization and ReLU activation function. The following equation shows the convolution layer's mathematical function.

$$X_s^l = \sum_{i,j} W_s^l X_{i,j}^{l-1} + B_s^l \tag{9}$$

Here, the outcome of current layer 'l' for 's' filter is denoted by X_s^l. $X_{i,j}^{l-1}$ Denotes the previous layer's output, the vertical and horizontal extent of filter is denoted by j and i correspondingly. B and W denote the bias and kernel. After the convolution layer, a batch normalisation is applied to normalise the input, and the transformation of the input is provided in the following equation.

$$\hat{X}^{l-1} = \frac{X^{l-1} - \mu}{\sqrt{\sigma^2 + \varepsilon}} \tag{10}$$

$$X^l = \alpha^l \hat{X}^{l-1} + \beta^l \tag{11}$$

Here, the shift parameters, learning rate, standard deviation and mean are denoted by $\beta, \alpha, \sigma, \mu$ correspondingly.

A ReLU activation function is provided in the following equation

$$\mathrm{Re}\,LU(X^l) = \max(0, X^l) \tag{12}$$

The convolution units are joined together to produce a fractal block with two columns using the join function. The equation (13) is used to calculate fractal blocks in a recursive manner.

$$Fb_{C+1}(N) = \left[(Fb_C \circ Fb_C)(N)\right] \oplus \left[conv(N)\right] \tag{13}$$

In the above equation, the no of columns is denoted by C, the join operation is denoted by $\oplus$ to calculate the mean of 2 convolution blocks and the composition is denoted by $\circ$. Several inputs are combined into a single output unit by the Join layer. From input to output, there are $2^C - 1$ convolution layers. To get a deeper network, this expansion rule is repeated. $2^C - 1$ is equals fractal block's depth. The fractal block with four columns has a depth of $2^4-1 = 15$ convolution units.

The feature vector is fed into the fractal block, which has a join layer and 3 convolution layers. The fractal block's output is given to the pooling layer, which decreases the feature map's dimension and the training parameters. The pooling layer and the fractal block sequence are repeated for five times. Finally, the fully connected layer obtained the features followed by the softmax classifier which classifies the classes of AD. To improve the performance of the classifier and reduce the error rate, the important parameters of Fractalnet such as learning rate, dropout rate and batch size are optimized by the Emperor penguin optimization algorithm.

3.4.1 Emperor Penguin Optimization:

The EPO technique is used to tune the hyper parameters of the Fractalnet model, which improves the classification performance of the proposed model. The purpose of parameter optimization is to alter the classifier's hyper parameters to the point where the classification performance is maximised.

The EPO algorithm is based on the huddling behaviour of emperor penguins (EPs) in Antarctica. Foraging is usually done in colonies by EPs. The huddling habit of the animals when foraging is an interesting characteristic. As a result, the primary goal is to decide a talented mover from the ground in a mathematically sound manner. Following the temperature profile θ', the distance between $EPs(X_{ep})$ is determined. For reaching optimal values, the effective mover is represented, and the positions of other EPs are changed. The following are the steps involved in EPO. The EPs' temperature profile is shown by

$$\theta' = (\theta - \frac{iter_{\max}}{C - iter_{\max}}) \tag{14}$$

$$\theta = \begin{cases} 0 & if\ Rn > 0.5 \\ 1 & if\ Rn < 0.5 \end{cases} \tag{15}$$

Here, C denotes the current round as determined by Iter max and Rn specifies the random number among 0 and 1: Because EPs tend to huddle together to maintain temperature, extra caution must be taken to safeguard them from nearby collisions. As a result, a set of two vectors $(\vec{V})$ and $(\vec{W})$ whose values are computed as follows:

$$\vec{V} = \{P \times (\theta' + X_{grid}(accuracy)) \times Rand0\} - \theta \tag{16}$$

$$\vec{W} = Rand() \tag{17}$$

$$X_{grid}(accuracy) = \left| \vec{X} - \vec{X}_{ep} \right| \tag{18}$$

Here, the best result is denoted by $\vec{X}$, $\vec{X}_{ep}$ denotes other EP's location, the movement parameter is represented by P, [0,1] and || is Rand's exact value.

$$\vec{D} = \left| \{S(\vec{V}).\vec{X}(x) - \vec{W}.\vec{X}_{ep}(x)\} \right| \tag{19}$$

$$S(\vec{V}) = \sqrt{(fe^{-C/v} - e^{-c})^2} \tag{20}$$

Eqs. (19) And (20) are used to calculate the distance among the EP and the optimal fittest searching agent. Eqs. (19) And (20) show the social forces that lead to EPs following the optimum searching agents, and e denotes the exponential function. The EPs' position can be upgraded based on the optimum agents obtained using Eq. (21).

$$\vec{X}_{ep}(X+1) = \vec{X}(x) - \vec{V}.\vec{D}_{ep} \quad (21)$$

The EP population is initialized in EPO using arbitrarily manufactured unique EPs.

4. Result and Discussion

This section provides a brief overview of the dataset utilised (ADNI) and assesses the efficacy of the proposed technique in various manner. Windows 10 operating system is used to train and test the proposed method with 16 GB of RAM and Anaconda navigator. Keras is used to run all of the simulations, with Tensorflow as the backend.

4.1 Dataset Description

The data is gathered from the AD Neuroimaging Initiative (ADNI) database (adni.loni.usc.edu), which has been utilised in a number of studies to classify Alzheimer's disease. Dr. Michael W. Weiner founded ADNI in 2004 with the aid of public-private collaboration. The basic goals of ADNI are to investigate more reliable and sensitive methodologies on various diagnostic tools, such as structural MRI, PET, MRI, and clinical assessment, in order to track the early stages of AD and course of MCI. 1296 MRI images are used in this study, divided into five categories: AD, LMCI, EMCI, MCI and NC.

4.2 Training and testing

The entire dataset is split into a training set (95%) and a testing set (5%). To train the segmentation and classification network, the SGD optimizer is employed. SGD can reach global minima and provide great training accuracy when using momentum. The number of columns in each fractal block in fractalNet is altered from 1 to 4. The training time of the network is increased when the number of columns increased. The model, on the other hand, provides improved accuracy for fractal blocks with two columns while requiring significantly less training time. As a result, the proposed model employs fractal blocks with two columns, each of which is repeated five times.

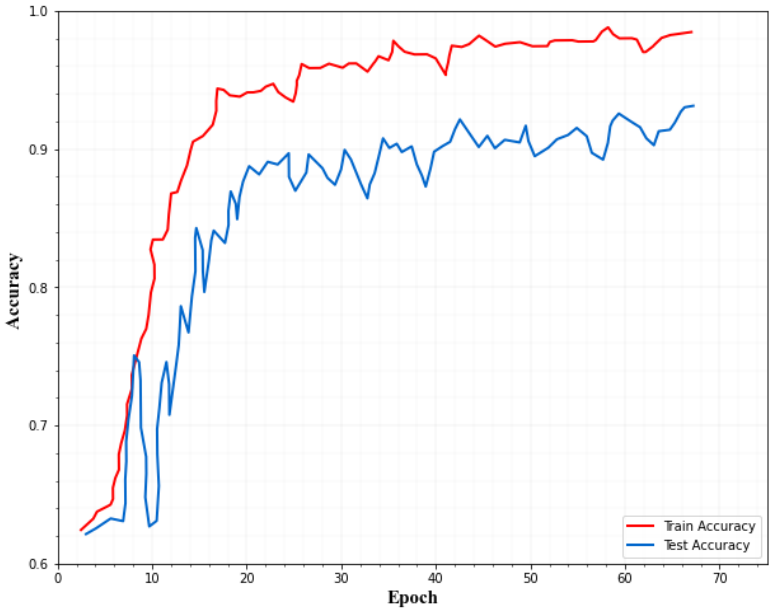

Figure 2: Training and testing accuracy for classification

The accuracy of the model is evaluated after it is applied to training data, and this is referred to as training accuracy. Testing accuracy is the accuracy when the testing data is applied to the model to obtain the result. As demonstrated in Fig. 2, the training and testing accuracy improves as the number of epoch's increases.

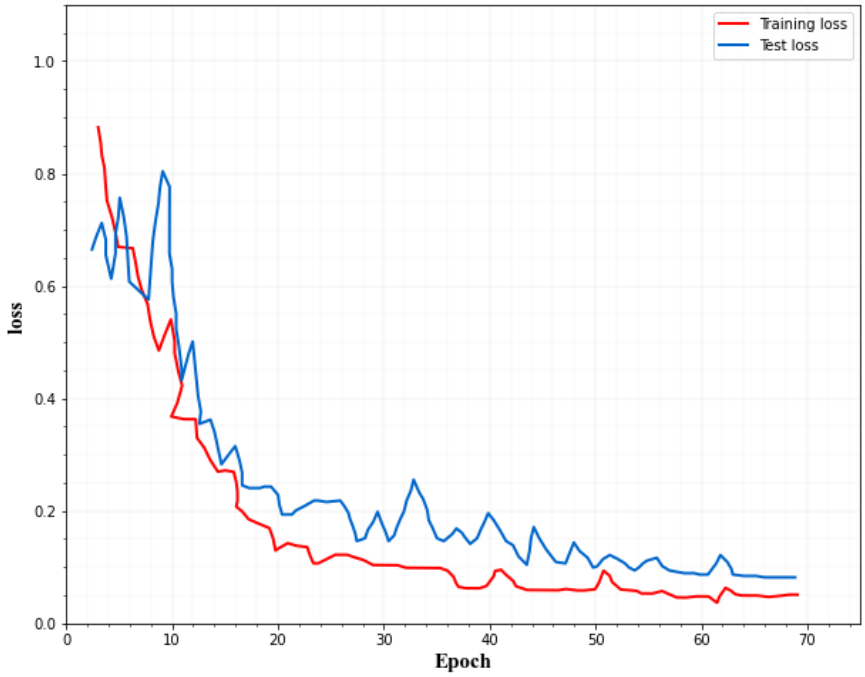

Figure 3: Training and testing Loss for classification

Both training and testing losses must be kept to a minimum. If the testing loss is greater than the training loss, the network is overfit. Overfitting can be reduced by using the optimization technique to increase each fractal block's drop out. Figure 3 illustrates that as the number of epochs rises, the training and testing error is decreased.

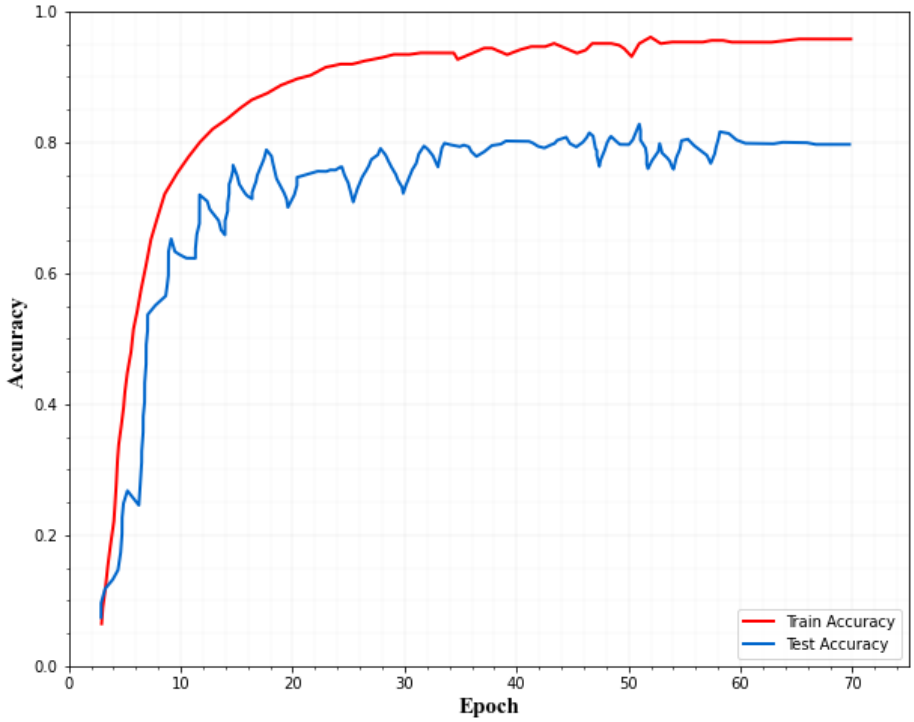

Figure 4: Training and testing accuracy for segmentation

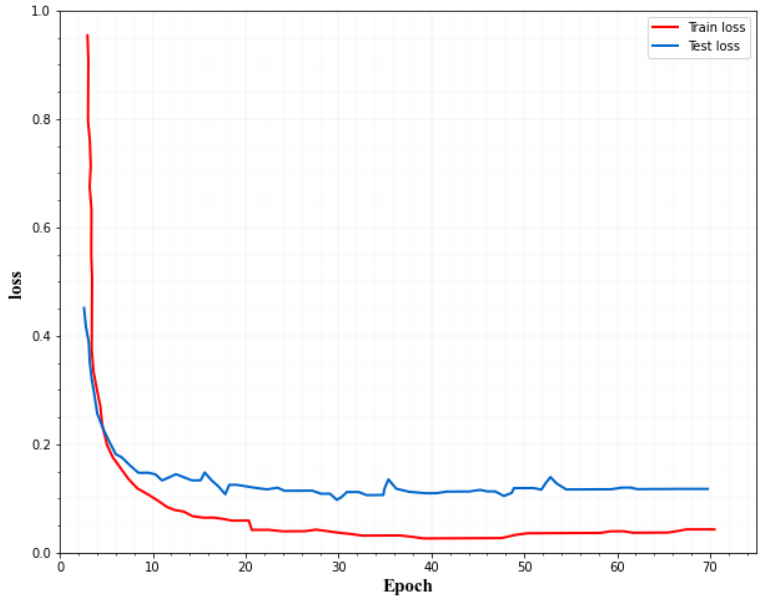

Figure 5. Training and testing loss for segmentation

Figure 4 and 5 shows the accuracy and loss curves of segmentation network. From the figures it is observed that the loss curve converges after 40 epochs and the accuracy curve converges after 20 epochs.

4.3 Segmentation results:

In this section, four variables are derived to assess segmentation performance: positive predicted value (PPV), sensitivity (SEN_S), and dice similarity coefficient (DSC).

$$DSC = \frac{2TPV}{FPV + FNV + 2TPV} \tag{22}$$

$$PPV = \frac{TPV}{TPV + FPV} \tag{23}$$

$$SEN\_S = \frac{TPV}{TPV + FNV} \tag{24}$$

Here, True positive pixels denotes TPV, False positive pixels denotes FPV and amount of false negative pixels denots FNV. The ratio of true positive pixels to the false negative pixels is denotes as sensitive (SEN_S).

The calculated results of the three assessment indexes come closer to showing superior segmentation effects. The quantitative results of segmentation technique are shown in table 1. From the table it is observed that the LMCI class achieves high DSC and SEN_s. The AD and EMCI classes are also achieves good performance. The graphical representation of this table is given in figure 6.

Table 1: The quantitative results of segmentation technique

Performance metrics	CN	MCI	EMCI	LMCI	AD
DSC	97.91	98.12	98.78	98.89	98.56
PPV	98.78	97.94	97.98	98.43	97.82
SEN-S	99.11	98.65	99.34	99.76	98.89

For the suggested approach, detailed assessments shows that the proposed method demonstrates its superiority in detecting significant object boundaries from brain MRI data. As a result, the phases of Alzheimer's disease can be detected more precisely.

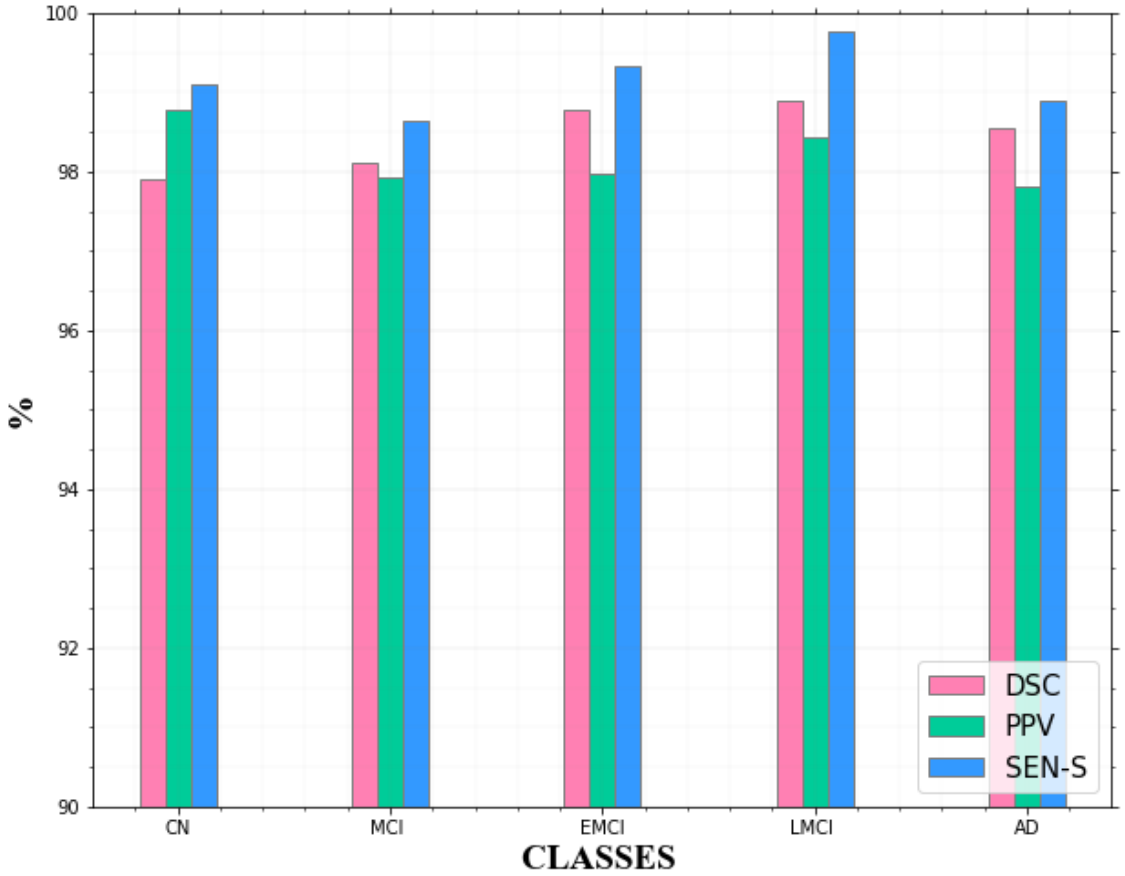

Figure 6: Comparison of segmentation metrics for AD classes

The suggested segmentation approach is compared to existing approaches in Table 2. When comparing the quantitative results of the various approaches listed in the table, it can be seen that the validation of the suggested system produced good results for brain segmentation. Using the proposed method, we achieve an DSC of 98.45%, PPV of 98.19%, and a Sensitivity of 99.15%. The graphical representation of the DSC metric comparison is given in figure 7.

Table 2: Comparison of proposed segmentation

Performance Metrics	CNN [28]	Gaussian Mixture Model [29]	U-NET [30]	k-means clustering [31]	Proposed
DSC	87.0	96.0	92.3	94.92	98.45
PPV	84.6	-	90.4	-	98.19
SEN-S	89.7	-	96.5	94.94	99.15

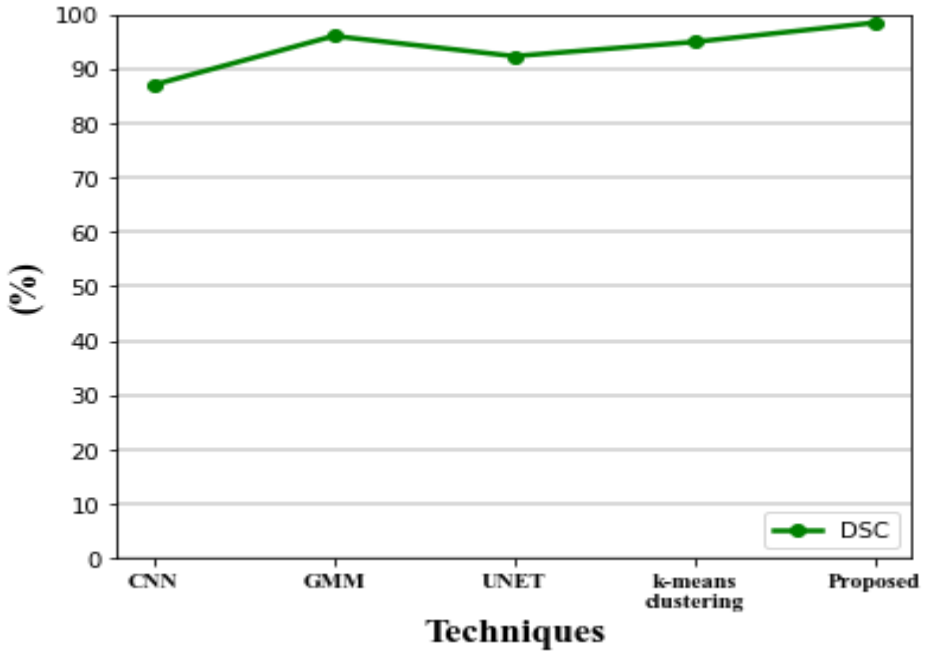

Figure 7: Comparison DSC metric with existing techniques

4.4 Classification results:

Experiments in this category track a variety of performance metrics. The accuracy of these metrics receives the most attention. The performance metrics used for classification are shown in the following equation.

$$Accuracy = \frac{TP + TN}{TP + TN + FP + FN} \tag{25}$$

The correct positive prediction's proportion is referred as recall. It is also called as true positive or sensitivity.

$$\text{Re}\,call = \frac{TP}{TP + FN} \tag{26}$$

The positive prediction's proportion called as precision as stated in the following equation,

$$\text{Pr}\,ecision = \frac{TP + TN}{TP + FP} \tag{27}$$

The curve formed by comparing True Positive Rate (TPR) vs False Positive Rate (FPR) is known as the receiver operating characteristic (ROC) curve.

$$TPR = \frac{TP}{TP + FN}, \qquad FPR = \frac{FP}{FP + TN}$$

In estimating classification performance, the AUC is a key metric.

Table 3: Evaluation results of proposed framework classes

metrics	CN	MCI	EMCI	LMCI	AD
Accuracy	99.16	99.21	99.69	98.45	98.81
Precision	99.47	100	100	100	99.13
recall	97.35	98.23	98.89	98.65	98.04
AUC	98.9	97.8	97.9	99.2	99.8

Table 3 summarizes the outcomes of our evaluation and Figure 8 illustrates the graphical representation of the five class's outcome. The confusion matrix of proposed approach is shown in figure 9. In the confusion matrix, the main diagonal contains major values. It means the majority of the images are correctly classified by the proposed approach.

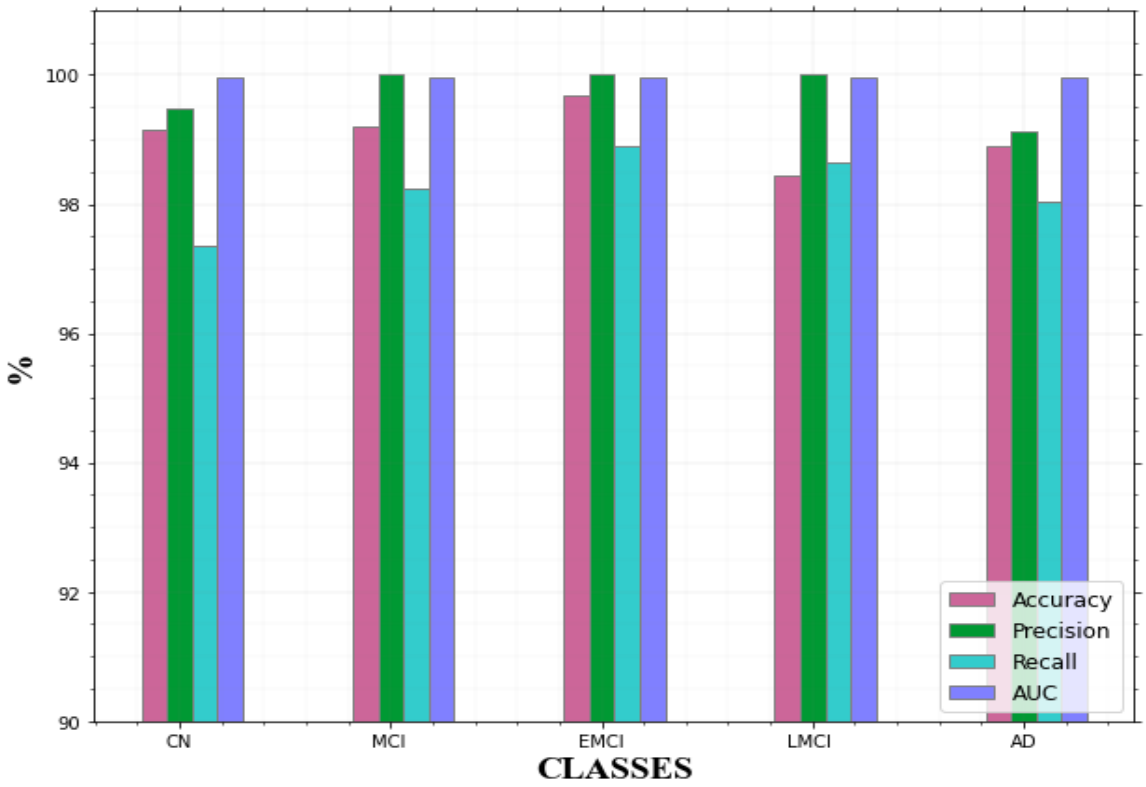

Figure 8: Comparison of AD classes

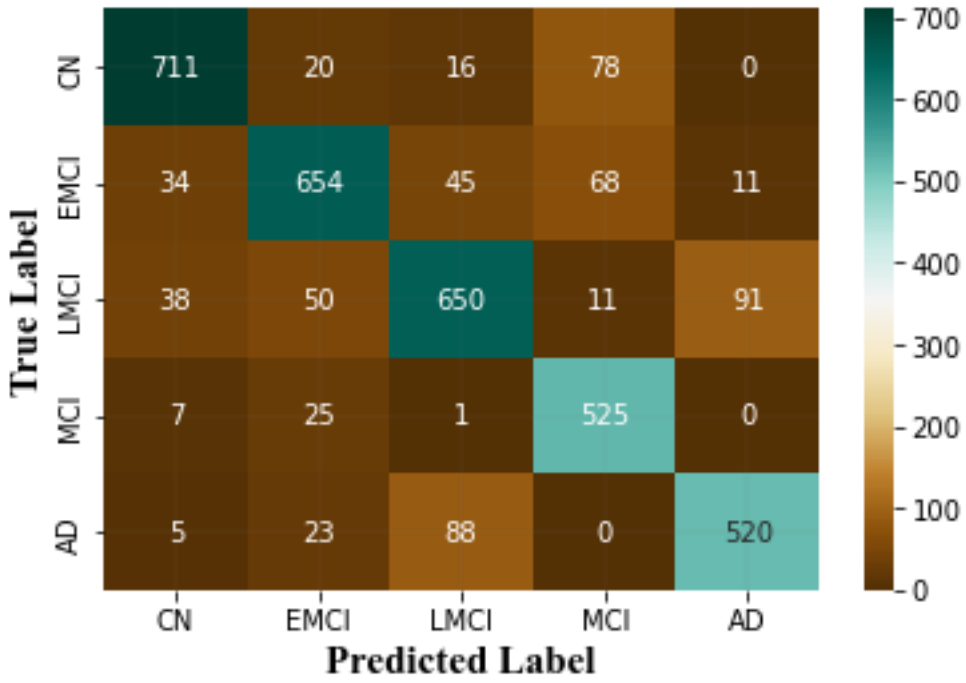

Figure 9: confusion matrix of proposed approach

These subcategories are utilized to identify the phases of AD. Each of the classes has features that show the existence of AD, although in varying degrees depending on the subclasses' dimensions. Figure 10 shows the ROC curves for these classes.

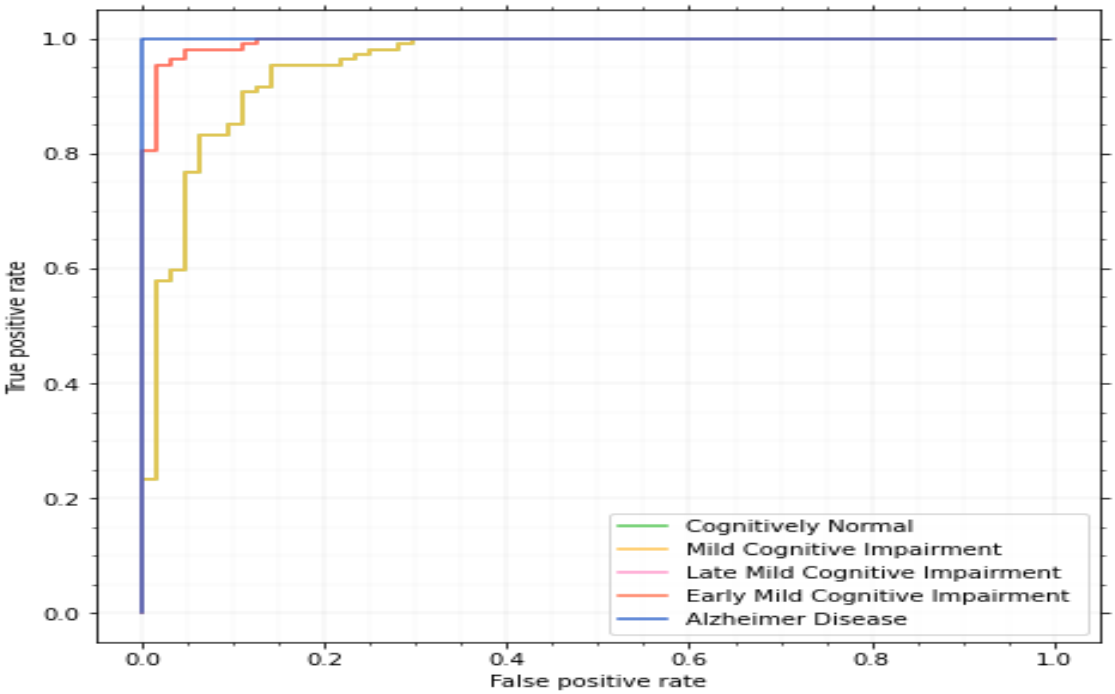

Figure 10: ROC curve of proposed approach

Each model's ROC curve is used to examine the classifier and is recognized a valuable tool. For CN, MCI, EMCI, LMCI, and AD, the ROC curve is 98.9, 97.8, 97.9, 99.2, and 99.8 respectively. The AUC score for AD is the highest, although other classes also do well.

Table 4: Comparison of proposed approach

Performance Metrics	Accuracy	Precision	recall	AUC
CNN [32]	95.2	-	94.6	97.2
Resnet-101 [21]	96.3	-	96.7	-
DSCNN [33]	75.32	-	80.13	81.41
Alexnet [34]	98.76	99.6	97.69	-
DEMNET [35]	95.23	96	95	97
3DCNN [36]	98.06	-	92.96	-
FCN [37]	96.8	-	95.7	-
Proposed	99.06	99.72	98.30	98.72

From table 4, it is observed that the deep separable convolutional neural network (DSCNN) attained the lowest accuracy for classification accuracy as 75.32%. The recall and the AUC of resnet-56 were 80.13% and 81.41% correspondingly. The accuracy of CNN, Dementia Network (DEMNET) and Resnet-101 seemed better than DSCNN but not good as fractalnet.

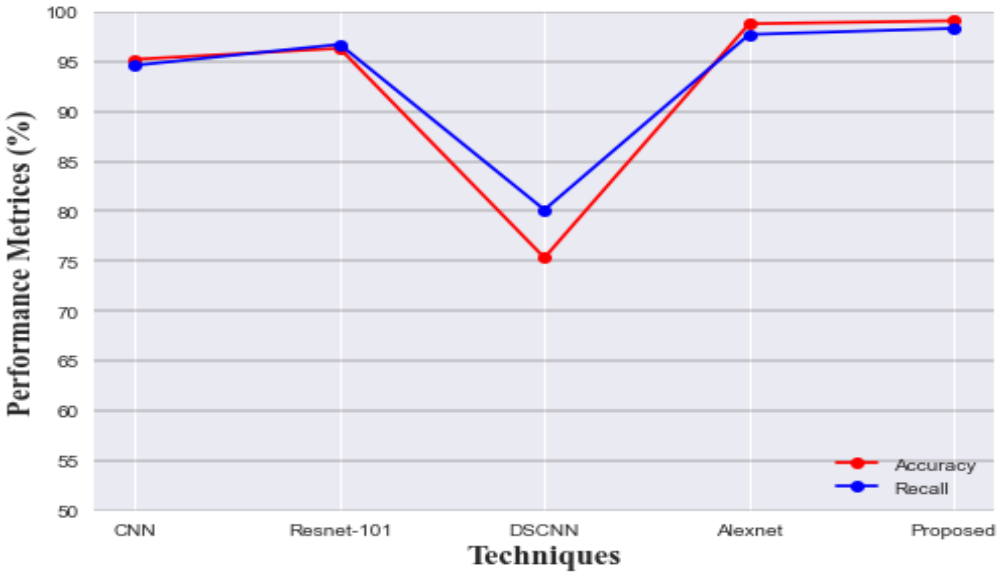

Figure 11: Comparison of Accuracy and recall of proposed with existing techniques

In terms of recall, Alexnet attains good performance and Dementia and FCN provides similar results. The accuracy, precision recall of fractalnet is better than the other four techniques. The alexnet's accuracy is 98.76% which is similar to fractalnet. Even though fractalnet is superior to alexnet in terms all metrics. The graphical representation of accuracy and recall comparison is given in figure 11. From all the above observation, it is understand that the proposed framework provides best performance to classify the AD which is really helpful for medical sector.

5. Conclusion:

AD is a serious neurological syndrome that affects a large portion of the global population. Early detection of AD is essential to improving the quality of people's lives and the development of better treatments and specialized medicines. The proposed framework was established to show the effectiveness of the deep learning algorithms to perform multi-class classification of AD and its various stages like LMCI, EMCI, MCI, CN and AD. Experiments on the ADNI dataset are used to examine the proposed method in depth. Furthermore, the findings of the proposed approach are compared with the existing methods and the experimental findings show that the model exceeds the competition and achieves an accuracy rate of 99.06%. In future, the proposed method could be utilized to identify lung and breast cancer.

Privacy and confidentiality

The respondent's right to privacy and confidentiality shall be protected in whatever way possible. The confidentiality of the respondent's information in its entirety was maintained at all times. The names and other identifying information of the people who participated in the research were not required for the analysis. The information that was submitted was identifiable by a code number and was handled with the utmost secrecy throughout the process. The identities of the respondents did not appear anywhere in the report of this research, nor were they referenced at any point.

Compensation

They were not paid or otherwise compensated for their participation in the research. All information provided by respondents was solely for the purpose of the research.

Funding

There is no financial support supplied by any organization.

Conflict of interest

The researchers vouch that there were no conflicts of interest involved in the study.

References:

1. Zhou, X., Qiu, S., Joshi, P. S., Xue, C., Killiany, R. J., Mian, A. Z., ...& Kolachalama, V. B. (2021). Enhancing magnetic resonance imaging-driven Alzheimer's disease classification performance using generative adversarial learning. Alzheimer's research & therapy, 13(1), 1-11.
2. Ferri, R., Babiloni, C., Karami, V., Triggiani, A. I., Carducci, F., Noce, G., ...& Arena, P. (2021). Stacked autoencoders as new models for an accurate Alzheimer's disease classification support using resting-state EEG and MRI measurements. Clinical Neurophysiology, 132(1), 232-245.
3. Divya, R., &ShanthaSelvaKumari, R. (2021). Genetic algorithm with logistic regression feature selection for Alzheimer's disease classification. Neural Computing and Applications, 33(14), 8435-8444.
4. Alinsaif, S., Lang, J., & Alzheimer's Disease Neuroimaging Initiative. (2021). 3D shearlet-based descriptors combined with deep features for the classification of Alzheimer's disease based on MRI data. Computers in Biology and Medicine, 138, 104879.
5. Helaly, H. A., Badawy, M., & Haikal, A. Y. (2022). Toward deep mri segmentation for alzheimer's disease detection. Neural Computing and Applications, 34(2), 1047-1063.
6. Balboni, E., Nocetti, L., Carbone, C., Dinsdale, N., Genovese, M., Guidi, G., ... & Zamboni, G. (2022). The impact of transfer learning on 3D deep learning convolutional neural network segmentation of the hippocampus in mild cognitive impairment and Alzheimer disease subjects. *Human Brain Mapping*.
7. Ansingkar, N. P., Patil, R., & Deshmukh, P. D. (2022). An efficient multi class Alzheimer detection using hybrid equilibrium optimizer with capsule auto encoder. *Multimedia Tools and Applications*, 1-32.
8. Ackah, J.Y., Amankwa-Danquah, P. and Atianashie, M.A., 2021. Religious noise pollution in Ghana: Source, effect and control. A Case Study of the Bono Region in Ghana. International Journal of Multidisciplinary Studies and Innovative Research, 5, pp.377-87.
9. Prabha, S., Sakthidasan@ Sankaran, K., & Chitradevi, D. (2021). Efficient optimization based thresholding technique for analysis of alzheimer MRIs. *International Journal of Neuroscience*, 1-14.
10. Allioui, H., Sadgal, M., & Elfazziki, A. (2021). Intelligent environment for advanced brain imaging: multi-agent system for an automated Alzheimer diagnosis. *Evolutionary Intelligence*, *14*(4), 1523-1538.
11. Nawaz, H., Maqsood, M., Afzal, S., Aadil, F., Mehmood, I., & Rho, S. (2021). A deep feature-based real-time system for Alzheimer disease stage detection. Multimedia Tools and Applications, 80(28), 35789-35807.
12. Atianashie Miracle A., Chukwuma Chinaza Adaobi, "Role of Digitalization in Balancing Work during Pandemic: Case of Microsoft," International Journal of Scientific Research in Computer Science and Engineering, Vol.10, Issue.2, pp.30-37, 2022.
13. Atianashie. Miracle. A. and J. K. . Odum, "Extrapolative Analytics of COVID-19 Pandemic: Arithmetical Modelling Perspective", SJST, vol. 3, no. 1, pp. 540–554, Feb. 2022.
14. Shanmugam, J. V., Duraisamy, B., Simon, B. C., & Bhaskaran, P. (2022). Alzheimer's disease classification using pre-trained deep networks. *Biomedical Signal Processing and Control*, *71*, 103217.
15. Goenka, N., & Tiwari, S. (2022). AlzVNet: A volumetric convolutional neural network for multiclass classification of Alzheimer's disease through multiple neuroimaging computational approaches. Biomedical Signal Processing and Control, 74, 103500.
16. Eroglu, Y., Yildirim, M., & Cinar, A. (2022). mRMR-based hybrid convolutional neural network model for classification of Alzheimer's disease on brain magnetic resonance images. *International Journal of Imaging Systems and Technology*, *32*(2), 517-527.
17. Atianashie. Miracle. A., "Implementation of Object Detection and Tracking by Using Deep Learning Based Convolutional Neural Networks", Scholars Journal of Science and Technology, vol. 3, no. 1, pp. 503–510, Feb. 2022.
18. Nagaraj, S., & Duong, T. Q. (2021). Deep Learning and Risk Score Classification of Mild Cognitive Impairment and Alzheimer's Disease. Journal of Alzheimer's Disease, 80(3), 1079-1090.
19. Zhou, X., Qiu, S., Joshi, P. S., Xue, C., Killiany, R. J., Mian, A. Z., ... & Kolachalama, V. B. (2021). Enhancing magnetic resonance imaging-driven Alzheimer's disease classification performance using generative adversarial learning. *Alzheimer's research & therapy*, *13*(1), 1-11.
20. Janghel, R. R., & Rathore, Y. K. (2021). Deep convolution neural network based system for early diagnosis of Alzheimer's disease. *Irbm*, *42*(4), 258-267.

21. Murugan, S., Venkatesan, C., Sumithra, M. G., Gao, X. Z., Elakkiya, B., Akila, M., & Manoharan, S. (2021). DEMNET: a deep learning model for early diagnosis of Alzheimer diseases and dementia from MR images. *IEEE Access*, *9*, 90319-90329.
22. Gao, X., Shi, F., Shen, D., & Liu, M. (2021). Task-induced Pyramid and Attention GAN for Multimodal Brain Image Imputation and Classification in Alzheimers disease. *IEEE Journal of Biomedical and Health Informatics*.
23. Buvaneswari, P. R., & Gayathri, R. (2021). Deep learning-based segmentation in classification of Alzheimer's disease. Arabian Journal for Science and Engineering, 46(6), 5373-5383.
24. AbdulAzeem, Y., Bahgat, W. M., &Badawy, M. (2021). A CNN based framework for classification of Alzheimer's disease. *Neural Computing and Applications*, *33*(16), 10415-10428.
25. Turkson, R. E., Qu, H., Mawuli, C. B., &Eghan, M. J. (2021). Classification of Alzheimer's disease using deep convolutional spiking neural network. *Neural Processing Letters*, *53*(4), 2649-2663.
26. Amini, M., Pedram, M., Moradi, A., &Ouchani, M. (2021). Diagnosis of Alzheimer's disease severity with fMRI images using robust multitask feature extraction method and convolutional neural network (CNN). *Computational and Mathematical Methods in Medicine*, *2021*.
27. Al-Adhaileh, M. H. (2022). Diagnosis and classification of Alzheimer's disease by using a convolution neural network algorithm. *Soft Computing*, 1-12.
28. Xu, Z., Deng, H., Liu, J., & Yang, Y. (2021). Diagnosis of Alzheimer 's disease Based on the Modified Tresnet. *Electronics*, *10*(16), 1908.
29. Basheera, S., & Ram, M. S. S. (2021). Deep learning based Alzheimer's disease early diagnosis using T2w segmented gray matter MRI. *International Journal of Imaging Systems and Technology*, *31*(3), 1692-1710.
30. Liu, M., Li, F., Yan, H., Wang, K., Ma, Y., Shen, L., ... & Alzheimer's Disease Neuroimaging Initiative. (2020). A multi-model deep convolutional neural network for automatic hippocampus segmentation and classification in Alzheimer's disease. Neuroimage, 208, 116459.
31. Tuan, T. A., Pham, T. B., Kim, J. Y., & Tavares, J. M. R. (2020). Alzheimer's diagnosis using deep learning in segmenting and classifying 3D brain MR images. International Journal of Neuroscience, 1-10.
32. Atianashie Miracle, A. and Adaobi, C.C., Cloud Computing In Health Care: Opportunities, Issues, And Applications: A Systematic Evaluation.
33. Yousefi-Banaem, H., & Malekzadeh, S. (2021). Hippocampus segmentation in magnetic resonance images of Alzheimer's patients using Deep machine learning. *arXiv preprint arXiv:2106.06743*.
34. Aaraji, Z. S., & Abbas, H. H. (2022). Automatic Classification of Alzheimer's disease using brain MRI data and deep Convolutional Neural Networks. *arXiv preprint arXiv:2204.00068*.
35. Atianashie Miracle, A., Armah, E.D.A. and Mohammed, N., A Portable Gui Based Sleep Disorder System Classification Based On Convolution Neural Networks (Cnn) In Raspberry Pi.
36. Basheera, S., & Ram, M. S. S. (2020). A novel CNN based Alzheimer's disease classification using hybrid enhanced ICA segmented gray matter of MRI. *Computerized Medical Imaging and Graphics*, *81*, 101713.
37. Liu, J., Li, M., Luo, Y., Yang, S., Li, W., & Bi, Y. (2021). Alzheimer's disease detection using depthwise separable convolutional neural networks. *Computer Methods and Programs in Biomedicine*, *203*, 106032.
38. Lee, B., Ellahi, W., & Choi, J. Y. (2019). Using deep CNN with data permutation scheme for classification of Alzheimer's disease in structural magnetic resonance imaging (sMRI). *IEICE TRANSACTIONS on Information and Systems*, *102*(7), 1384-1395.
39. Murugan, S., Venkatesan, C., Sumithra, M. G., Gao, X. Z., Elakkiya, B., Akila, M., & Manoharan, S. (2021). DEMNET: a deep learning model for early diagnosis of Alzheimer diseases and dementia from MR images. IEEE Access, 9, 90319-90329.
40. Atianashie Miracle, A. and Opoku, M., 2021. Patterned De-Duplication On Dependable Data Subcontracting With Three Error Detecting Techniques On Cloud Computing.
41. Qiu, S., Joshi, P. S., Miller, M. I., Xue, C., Zhou, X., Karjadi, C., ... & Kolachalama, V. B. (2020). Development and validation of an interpretable deep learning framework for Alzheimer's disease classification. *Brain*, *143*(6), 1920-1933.